



ELSEVIER

Contents lists available at ScienceDirect

Comptes Rendus Chimie

www.sciencedirect.com



Full paper/Mémoire

# Synthesis, structural characterization and reactivity of manganese tungstate nanoparticles in the oxidative degradation of methylene blue

Mostafa Khaksar<sup>a</sup>, Davar M. Boghaei<sup>a,\*</sup>, Mojtaba Amini<sup>b,\*</sup><sup>a</sup> Chemistry Department, Sharif University of Technology, P.O. Box 11155-3615, Tehran, Iran<sup>b</sup> Department of Chemistry, Faculty of Science, University of Maragheh, P.O. Box. 55181-83111, Maragheh, Iran

## ARTICLE INFO

## Article history:

Received 3 February 2014

Accepted after revision 17 April 2014

Available online 26 November 2014

## Keywords:

Nanoparticle

MnWO<sub>4</sub>

Methylene blue

TBHP

## ABSTRACT

Nanoparticles of manganese tungstate (MnWO<sub>4</sub>) were prepared via an impregnation method using Mn(NO<sub>3</sub>)<sub>2</sub>·4H<sub>2</sub>O and WO<sub>3</sub> as a source of Mn and W, respectively. The morphology of the manganese tungstate nanoparticles was studied in detail by X-ray diffraction (XRD), scanning electron microscopy (SEM) and transmission electron microscopy (TEM). MnWO<sub>4</sub> nanoparticles showed severe catalytic performances for the degradation of organic dye (methylene blue, MB) in the presence of *tert*-butyl hydrogen peroxide, TBHP, as the oxidant at room temperature in water.

© 2014 Académie des sciences. Published by Elsevier Masson SAS. All rights reserved.

## 1. Introduction

Organic dyes play a major role in not only the traditional textile and dyeing industries, but also in new areas such as food, pharmaceutical, cosmetics, imaging biological samples, liquid crystals, lasers, solar cells, optical data discs and computer industries [1–3]. The developed applications of these dyes are mostly based on color changes. Using these dyes produces a great deal of dye wastes, which cause significant environmental problems, due to the fact that the dyes are highly colored, designed to resist chemical, biochemical and photochemical degradation [4–6]. Therefore, the removal of dyes from waste effluents has attracted much attention in the field of environmental chemistry [7,8].

Recent advances in the synthesis and characterization of nano-sized materials have promoted extensive

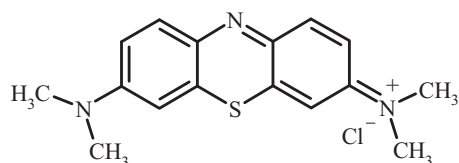
researches dealing with methods of preparation of highly efficient nanostructured catalysts for dye removal from water streams with the combined effect of hydrogen peroxide as an oxidant [9–12]. Supported noble metal oxides and mixed metal oxides have been widely employed in the catalytic oxidation of organic dyes [13,14].

Manganese tungstate (MnWO<sub>4</sub>) is a promising material with potential applications in many fields, such as photoluminescence [15], humidity sensors [16], magnetic materials [17], photo catalysts [18], etc. MnWO<sub>4</sub> is a cheap, environmentally friendly material and could be prepared as nano-sized particles with large surface area, and thus many of their active sites are accessible to the reactants. It is well known that the morphology and the size have extensive influence on the physical and chemical properties of MnWO<sub>4</sub> [19]. Hence, synthesis of MnWO<sub>4</sub> nano/microstructures with different morphologies has become a target in the reported researches.

Therefore, herein we report the preparation of MnWO<sub>4</sub> nanoparticles as efficient catalysts for the green decomposition of methylene blue (MB) using *tert*-butyl hydrogen peroxide (TBHP) as the oxidant (Scheme 1). The extent of

\* Corresponding authors.

E-mail addresses: [dboghaei@sharif.edu](mailto:dboghaei@sharif.edu) (D.M. Boghaei), [mamini@maragheh.ac.ir](mailto:mamini@maragheh.ac.ir) (M. Amini).



Scheme 1. Structure of methylene blue (MB).

dye decomposition was monitored using UV-Vis spectroscopy technique.

## 2. Experimental

### 2.1. Materials

All reagents and solvents were purchased from commercial sources and were used without further purification.

### 2.2. Characterization

Transmission electron microscopy (TEM) was conducted on carbon-coated copper grids using a FEI Technai G2 F20 Field Emission scanning transmission electron microscope (STEM) at 200 kV (point-to-point resolution  $< 0.25$  nm, line-to-line resolution  $< 0.10$  nm). The TEM samples were prepared by placing 2–3 drops of dilute ethanol solutions of the nanomaterials onto carbon-coated copper grids. SEM was carried out with Philips CM120 and LEO 1430VP instruments. The pH of zero point charge,  $\text{pH}_{\text{ZPC}}$ , was determined by acid–base titration according to Davranche et al. [20]. The X-ray powder patterns were recorded with a Bruker D8 ADVANCE (Germany) diffractometer (Cu  $\text{K}\alpha$  radiation). Absorption spectra were recorded by a CARY 100 Bio VARIAN UV–vis spectrophotometer. FT–IR spectra were obtained by using a Unicam Matson 1000 FT-IR spectrophotometer using KBr disks at room temperature.

### 2.3. Synthesis of $\text{MnWO}_4$ nanoparticles

An aqueous solution ( $10 \text{ cm}^3$ ) of  $\text{Na}_2\text{WO}_4 \cdot 2\text{H}_2\text{O}$  (0.825 g; 2.5 mmol) was acidified with HCl solution ( $1 \text{ cm}^3$ , 6 M), and a white precipitate of  $\text{WO}_3 \cdot n\text{H}_2\text{O}$  (0.69 g) was obtained [21]. Then a solution of  $\text{Mn}(\text{NO}_3)_2 \cdot 4\text{H}_2\text{O}$  (2.5 mmol) in 20 mL of deionized water was added to the obtained  $\text{WO}_3 \cdot n\text{H}_2\text{O}$ . This mixture was mechanically stirred and then  $\text{H}_2\text{O}$  was evaporated under vacuum using a rotary evaporator. After the third evaporation process, the left solid was ground and calcined at  $300^\circ\text{C}$  for 6 h in the air.

### 2.4. Methylene blue degradation

The catalytic activity of the manganese tungstate nanoparticles was demonstrated by degrading MB in aqueous solution. First, a stock solution of aqueous MB (10 mg/L) was prepared. Fifty milliliters of aqueous MB were poured into a round-bottom flask, and 10 mg of catalyst were added to it. 0.1 mol of oxidant (TBHP) was added to the reaction mixture and was allowed to react in ambient conditions under stirring. For a given time interval, a small quantity of the mixture solution was pipetted into a quartz cell and its absorption spectrum was measured by a UV–visible spectrophotometer.

## 3. Results and discussion

### 3.1. Catalyst characterization

In order to confirm the crystalline structure of the prepared  $\text{MnWO}_4$ , the XRD study was carried out (Fig. 1). According to the XRD pattern, pure crystalline  $\text{MnWO}_4$  was obtained. All reflection peaks of the product can be easily indexed as a pure, monoclinic wolframite tungstate structure with space group  $P2_1/c$ , and the cell parameters of  $\text{MnWO}_4$  were as follows:  $a = 0.48277$  nm,  $b = 0.57610$  nm,  $c = 0.49970$  nm,  $\alpha = \gamma = 90^\circ$  and  $\beta = 91.14^\circ$ , which is consistent with values taken from the literature (JCPDS Card

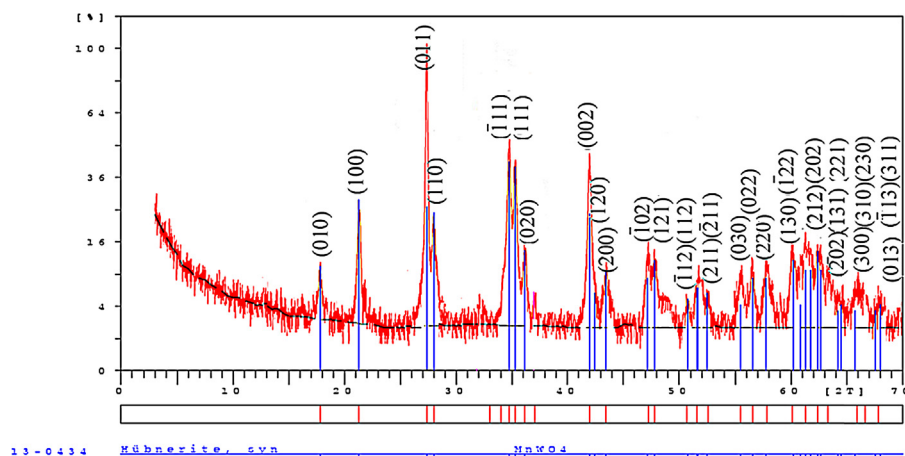


Fig. 1. (Color online.) XRD pattern of  $\text{MnWO}_4$  nanoparticles; blue line: XRD parameters of reported  $\text{MnWO}_4$  catalyst (JCPDS Card Number: 80-0133) and red line: XRD parameters of prepared  $\text{MnWO}_4$  catalyst in the present work.

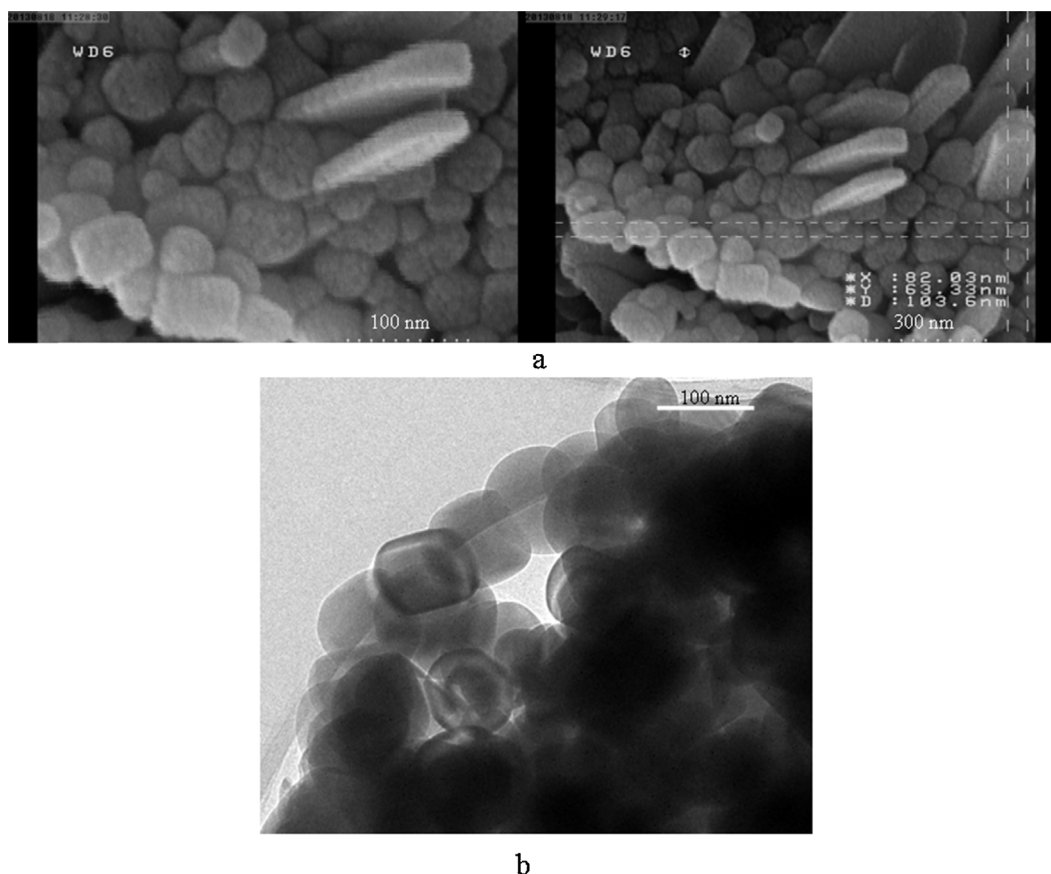


Fig. 2. (a) SEM and (b) TEM images of  $\text{MnWO}_4$ .

Number: 80-0133) [22]. The sharpness of the diffraction peaks also indicates the high crystallinity of  $\text{MnWO}_4$ . Moreover, the main reflection peaks of all pure  $\text{MnWO}_4$  have a trend to shift to low angles slightly compared to standard cards (on abscissa axis), which illustrates the increase in cell parameters.

To characterize the morphology of the prepared oxides, they were studied by scanning electron microscopy (SEM) and transmission electron microscopy (TEM). SEM and TEM images are shown in Fig. 2. The SEM images presented in Fig. 2a indicate the growth of sphere-like  $\text{MnWO}_4$  crystals.

The TEM image of  $\text{MnWO}_4$  shows approximately monodispersed nanocrystalline  $\text{MnWO}_4$  particles with diameters of ca. 70–100 nm (Fig. 2b).

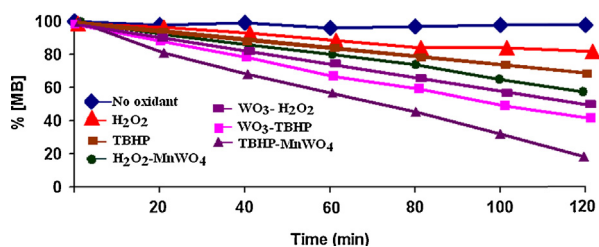


Fig. 3. (Color online.) Percentage decomposition of MB in the presence of various oxidants.

### 3.2. Catalytic effects

The decrease in percentage of dye concentration is a reliable criterion for the activity of the catalysts during the reaction, which is proportional to the disappearance of the dye color.

A plot of percentage decrease in [MB] versus time represents the influence of the oxidant on the decomposition of MB dye catalyzed by  $\text{MnWO}_4$  nanoparticles at room temperature (Fig. 3). As it is shown, the removal of MB was not observed when only  $\text{H}_2\text{O}_2$  or TBHP was added into the MB solution, which indicates that the direct oxidation of MB by  $\text{H}_2\text{O}_2$  or TBHP was very limited and that no dye decomposition was observed, even after 120 min.

The effect of the TBHP amount on the percentage decomposition of MB was studied, and the results are

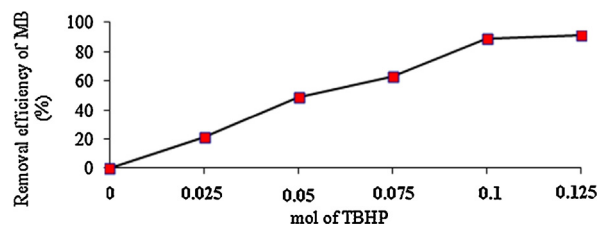


Fig. 4. Effects of the amount of TBHP on the percentage decomposition of MB.

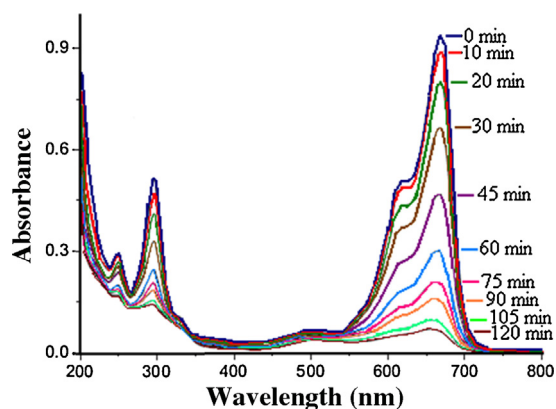


Fig. 5. (Color online.) Changes in the UV-vis absorbance spectra of MB dye using  $\text{MnWO}_4$  catalyst with TBHP in 120 min.

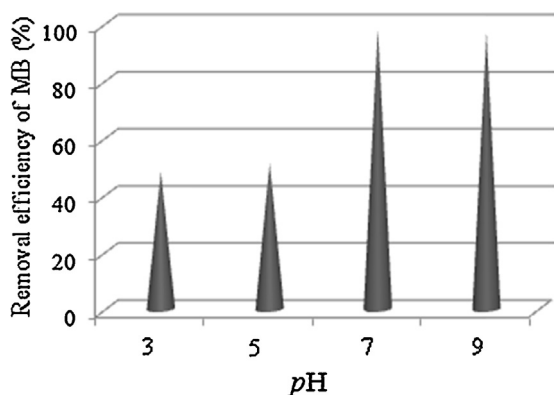


Fig. 6. Effects of pH on the degradation of MB in the presence of  $\text{MnWO}_4$ .

shown in Fig. 4. When the amount of TBHP varies from 0 to 0.1 mol, the percentage decomposition of MB increased from 0 to ca. 90%.

When the  $\text{MnWO}_4$  catalyst was added to a MB solution containing TBHP, the removal of MB was slightly increased, relative to the case when TBHP was alone in the system. However, as shown in Fig. 5, MB could be completely removed after 120 min in the presence of the catalyst and of TBHP, showing that  $\text{MnWO}_4$  facilitates the oxidation of MB by TBHP. Although the use of  $\text{WO}_3$  in the presence of TBHP can have a good influence on dye decomposition, our

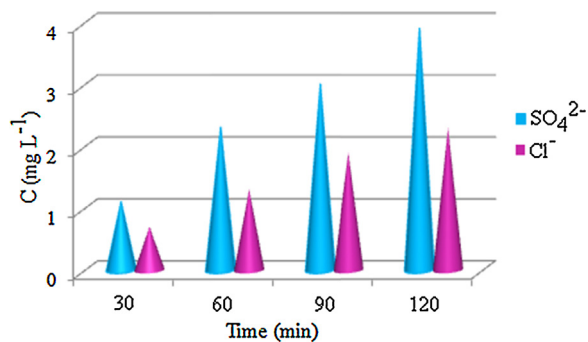


Fig. 8. (Color online.) The production of  $\text{SO}_4^{2-}$  and  $\text{Cl}^-$  ions from MB ( $50 \text{ mg L}^{-1}$ ) degradation at a reaction time of 120 min in the presence of  $\text{MnWO}_4$ .

proposed method decomposes MB much more efficiently (Fig. 3).

It has been well established that the oxidative degradation of organic matter by metal oxides is accomplished via a surface mechanism [23], that is, the organic compound is adsorbed on the surface of metal oxides to form a surface precursor complex, then electron transfer occurs within the surface complex from the organic reductant to the surface-bound metal, followed by the release of organic oxidation products. The formation of a surface precursor complex is one of the kinetic rate-limiting steps in the heterogeneous oxidative degradation of organic pollutants, closely related to the nature of the surface charge.

The effect of pH on the degradation efficiency of MB was examined in the range from 3 to 9. As illustrated in Fig. 6, MB degradation worked very effectively over a wide pH range from 3 to 9, which is very favorable to the practical treatment of wastewater, since there is no need to adjust the solution pH. After 2 h, 51% of MB was degraded at pH 5 and an almost complete degradation occurred in neutral and alkaline solutions. The effect of pH on the catalytic reaction can be mainly explained by the surface charge of  $\text{MnWO}_4$  (point of zero charge,  $\text{pH}_{\text{pzc}}$  of  $\text{MnWO}_4 \sim 6.3$ ). In aqueous solution, at pH values below 6.3, the catalyst's surface is positively charged and, above pH 6.3, it is negatively charged. Being a cationic dye, MB would prefer to adsorb on the negative surface. However, about 48% of MB can be degraded when the pH value of the solution approaches 3.

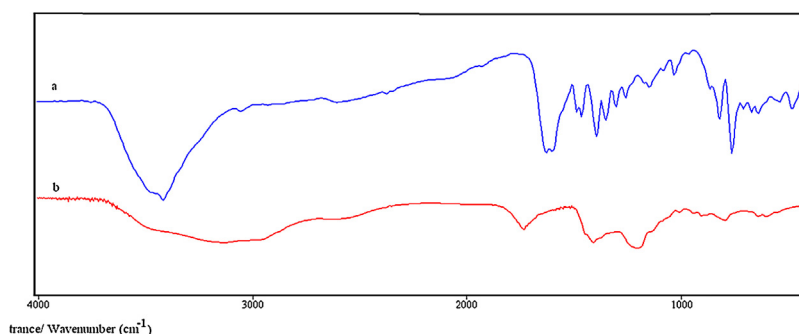


Fig. 7. Changes in the FT-IR spectrum of MB during degradation.

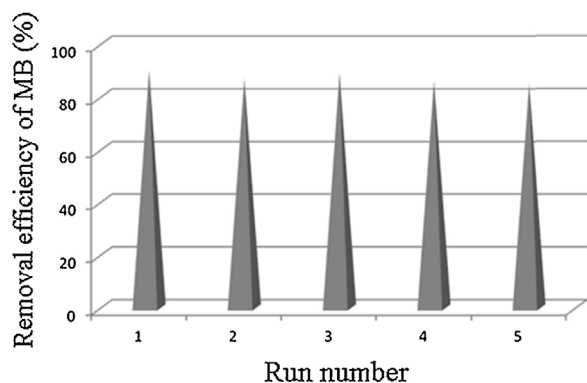


Fig. 9. Recycling studies of the MnWO<sub>4</sub> catalyst in the degradation of MB.

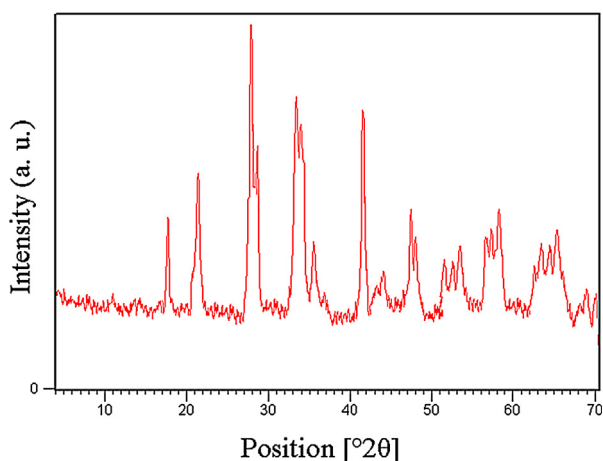


Fig. 10. (Color online.) XRD pattern of the used catalyst.

Fig. 7 shows the changes in the FT-IR spectrum of MB in the presence of a catalyst as a function of the reaction time. In curve a, the peaks at 1611 and 1407  $\text{cm}^{-1}$  are assigned to the C=N and C-N bonds in the heterocycle of MB, respectively. As shown in curve b, these characteristic peaks have disappeared during the reaction time. Meanwhile, the appearance of new peaks at 1641, 1350 and 1210  $\text{cm}^{-1}$ , attributed to the stretching vibrations of N=O, N-O, and S=O bonds, can be seen.

It has been established that the complete oxidative degradation of methylene blue produces  $\text{CO}_2$ ,  $\text{HNO}_3$ ,  $\text{H}_2\text{SO}_4$  and HCl [23]. In our system,  $\text{H}_2\text{SO}_4$  and HCl were determined gravimetrically by precipitating them respectively as  $\text{BaSO}_4$  and  $\text{AgCl}$ , using  $\text{BaCl}_2$  and  $\text{AgNO}_3$  as precipitants. As shown in Fig. 8, the  $\text{SO}_4^{2-}$  and  $\text{Cl}^-$  concentrations increased with increasing the degradation time.

Finally, the effect of repeated uses of the catalyst on its catalytic activity was examined. After the end of the first experiment, the catalyst was washed with bi-distilled water, dried and a new experiment was started. The results

in Fig. 9 demonstrate that about 90% of MB removal is accomplished after a five-cycle run in the presence of the  $\text{MnWO}_4$  catalyst. It should be noted that the catalytic activity of the catalyst is almost unaffected upon repeated use.

We also found that the XRD patterns of both fresh and used catalysts are very similar (Fig. 10). The results show that the catalyst did not undergo any change during the reaction.

#### 4. Conclusion

The  $\text{MnWO}_4$  nanoparticles were successfully synthesized using an impregnation method. Experimental results from this economical and environmentally friendly study showed that MB dye was successfully decomposed using  $\text{MnWO}_4$  as a catalyst. The effects of the oxidant, of time and of pH on the degree of decomposition of the MB dye were also studied.

#### Acknowledgements

M. Amini thanks the Research Council of the University of Maragheh for financial support of this work.

#### References

- [1] P. Bautista, A.F. Mohedano, J.A. Casas, J.A. Zazo, J.J. Rodriguez, *J. Chem. Technol. Biotechnol.* 83 (2008) 1323.
- [2] Aihua Xu, Xiaoxia Li, Shuang Ye, Guochuan Yin, Zeng. Qingfu, *Appl. Catal. B: Environ.* 102 (2011) 37.
- [3] S. Caudo, G. Centi, C. Genovese, S. Perathoner, *Top. Catal.* 40 (2006) 207.
- [4] M.S. Lucas, J.A. Peres, J. Hazard. Mater. 168 (2009) 1253.
- [5] J.M. Monteagudo, A. Durán, C. López-Almodovar, *Appl. Catal. B* 83 (2008) 46.
- [6] A.H. Xu, H. Xiong, G.C. Yin, *J. Phys. Chem. A* 113 (2009) 12243.
- [7] H.A. Le, L.T. Linh, S. Chin, J. Jürg, *Powder Technol.* 225 (2012) 167.
- [8] O. Impart, A. Katafias, P. Kita, A. Mills, A. Pietkiewicz-Graczyk, G. Wrzeszcz, *Dalton Trans.* 2003 (2003) 348.
- [9] V.K. Garg, M. Amita, R. Kumar, R. Gupta, *Dyes Pigments* 63 (2004) 243.
- [10] T. Sriskandakumar, N. Opembe, C.-H. Chen, A. Morey, C. Kin?ondu, S.L. Suib, *J. Phys. Chem. A* 113 (2009) 1523.
- [11] M.U. Anu Prathap, B. Kaur, R. Srivastava, *J. Colloid Interf. Sci.* 370 (2012) 144.
- [12] H. Wang, Y. Huang, *J. Hazard. Mater.* 191 (2011) 163.
- [13] C.S. Castro, M.C. Guerreiro, L.C.A. Oliveira, M. Gonçalves, A.S. Anastácio, M. Nazzarro, *Appl. Catal. A: Gen.* 367 (2009) 53.
- [14] K.A.M. Ahmed, H. Peng, K. Wu, K. Huang, *Chem. Eng. J.* 172 (2011) 531.
- [15] M.A.P. Almeida, L.S. Cavalcante, J.A. Varela, M. Siu Li, E. Longo, *Adv. Powder Technol.* 23 (2012) 124.
- [16] W. Qu, W. Wlodarski, J.U. Meyer, *Sensor Actuat. B Chem.* 64 (2000) 76.
- [17] F. Ye, R.S. Fishman, J.A. Fernandez-Baca, A.A. Podlesnyak, G. Ehlers, H.A. Mook, Y.Q. Wang, B. Lorenz, C.W. Chu, *Phys. Rev. B* 83 (2011) 140401.
- [18] W.Q. Wu, W.H. Qin, Y.M. He, Y. Wu, T.H. Wu, *J. Exp. Nanosci.* 7 (2012) 390.
- [19] U. Dellwo, P. Keller, J.U. Meyer, *Sensor. Actuat. A Phys.* 61 (1997) 298.
- [20] M. Davranche, S. Lacour, F. Bordas, J.-C. Bollinger, *J. Chem. Educ.* 80 (2003) 76.
- [21] N. Gharah, S. Chakraborty, A.K. Mukherjee, R. Bhattacharyya, *Inorg. Chim. Acta* 362 (2009) 1089.
- [22] S. Zhou, J. Huangn, T. Zhang, H. Ouyang, A. Li, Z. Zhang, *Ceram. Int.* 39 (2013) 5159.
- [23] I.A. Salem, M.S. El-Maazawi, *Chemosphere* 41 (2000) 1173.